J. Am. Ceram. Soc., **87** [2] 296–98 (2004)

Mullite–Boron Nitride Composite with High Strength and Low Elasticity

G. J. Zhang,[★,†] J. F. Yang,[★,‡] M. Ando,[†] T. Ohji,[★,‡] and S. Kanzaki[★,‡]

Synergy Ceramics Laboratory, Fine Ceramics Research Association, Nagoya, Aichi 463-8687, Japan

Synergy Materials Research Center, National Institute of Advanced Industrial Science and Technology, Nagoya, Aichi 463-8687, Japan

Mullite–boron nitride (BN) composite with high strength, low Young's modulus, and highly improved strain tolerance was prepared by reactive hot pressing (RHP) using aluminum borates ($9Al_2O_3{\cdot}2B_2O_3$ and $2Al_2O_3{\cdot}B_2O_3$) and silicon nitride as starting materials. Compared with the monolithic mullite, the composite RHPed at 1800°C showed 1.64 times (540 MPa) the strength, 70% (153 GPa) the Young's modulus, and 2.34 times (3.53×10^{-3}) the strain tolerance. Transmission electron microscopy observation revealed that the composite had an isotropic microstructure with a fine mullite matrix grain size of less than 1 μm and nanosized hexagonal BN (h-BN) platelets of about 200 nm in length and 60–80 nm in thickness. The high strength was suggested to be from the reduced matrix grain size and the small toughening effect by the h-BN platelets.

I. Introduction

Mullite monolithic ceramics demonstrate moderate strength and elasticity, low thermal expansion coefficient, and good resistance to thermal shock and creep.[1–3] For structural applications, however, its strength and fracture toughness need to be improved. Some composite systems, formed mainly by adding high-strength second-phase reinforcements such as ZrO_2, Al_2O_3, SiC, and Mo, etc., have been reported.[4–10] Compared with those of mullite monolithic ceramics, the composite strength has been improved from 300–400 to 500–600 MPa and fracture toughness from 2–3 to 4–7 $MPa{\cdot}m^{1/2}$. On the other hand, however, those composites also show high elasticity. For improvement in the thermal shock resistance or avoidance of high stress at the joining section of ceramic parts when applied by joining with metals that possess relative low elasticity, we need to decrease the elasticity of these ceramics.

In recent years we have been trying to design and fabricate materials with high strength and low elasticity (thus improving strain tolerance) by incorporating second phases of low Young's-modulus-like pores (here we regard the pore as a second phase of zero Young's modulus) and hexagonal boron nitride (h-BN). Through control of the volume fraction, size, shape, distribution, and oriented alignment of the second phase, a series of materials with high strain tolerance have been developed.[11–16] From these investigations we find that the reaction synthesis is an effective approach to prepare high-strain-tolerant materials because of the resulting strong bonding between the in-situ-formed grains.

Mullite–BN composites have been prepared through the reaction of B_2O_3, Si_3N_4, and AlN.[17] However, there are problems in processing due to the moisture-sensitive, low melting point and easy evaporation of B_2O_3. Recently we successfully synthesized Al_2O_3–BN composites with high mechanical properties by using aluminum borates ($9Al_2O_3{\cdot}2B_2O_3$ and $2Al_2O_3{\cdot}B_2O_3$) and aluminum nitride (AlN) as reactants.[18] The aluminum borates do not melt at low temperature and are water-resistant. In this study, a new reactive approach is proposed to synthesize mullite–BN composites by using aluminum borates and Si_3N_4 as reactants:

$$0.2(9Al_2O_3{\cdot}2B_2O_3) + 3.6(2Al_2O_3{\cdot}B_2O_3) + 2Si_3N_4 = 3(3Al_2O_3{\cdot}2SiO_2) + 8BN \quad (1)$$

The calculated volume percent of BN in the synthesized composite is 17.83% using the theoretical density values of 3.17 g/cm^3 for mullite and 2.27 g/cm^3 for BN.[13] This paper will report the mechanical properties and microstructure of the mullite–BN composite synthesized by reactive hot pressing (RHP).

II. Experimental Procedure

The starting materials used were $9Al_2O_3{\cdot}2B_2O_3$ (9A2B; mean particle size, D50 = 2.36 μm; BET specific surface, A_s = 9.89 m^2/g; Shikoku Chemical Co., Marugame-shi, Japan), $2Al_2O_3{\cdot}B_2O_3$ (2AB; D50 = 2.85 μm; A_s = 27.91 m^2/g; Shikoku Chemical Co.), Si_3N_4 (E-10 grade; D50 = 0.5 μm; Ube Industries, Yamaguchi, Japan), and mullite (KM102; D50 = 0.74 μm; A_s = 8.4 m^2/g; Kyoritsu Materials Co., Nagoya, Japan). The stoichiometric powders were mixed in ethanol with Al_2O_3 balls for 72 h in a plastic bottle and then dried. The powder mixture was RHPed under a pressure of 30 MPa in a BN-coated graphite die at 1600°, 1700°, and 1800°C, respectively, for 60 min in an argon atmosphere. At temperatures of lower than 600°C, a vacuum of about 10^{-4} torr was maintained in the furnace. Then, Ar gas was added into the chamber up to a pressure of 1.3 atm, and the pressure used for hot pressing was gradually increased to 30 MPa. The heating rate was 10°C /min. For comparison, a mullite monolithic ceramic was prepared by hot pressing at 1700°C for 60 min in an argon atmosphere.

The obtained hot-pressed products had dimensions of 42 mm × 45 mm × 6 mm. Specimens of 3 mm × 4 mm × 42 mm in dimensions were cut from them and then ground and beveled with a diamond wheel of 600-grit size. The density was tested using the water-displacement method. The phase composition was determined by X-ray diffraction (XRD) using Cu*K*α radiation. The three-point bending strength was measured with the span of 30 mm and a crosshead speed of 0.5 mm/min. The strength values were an average of five measurements. The fracture toughness was measured by the indentation method using a 5-kg load.[19] However, a load of 2 kg was used for mullite monolithic ceramics due to chipping that always occurred around the indent if a 5-kg load was applied. The data of hardness and toughness were an average of 10 measurements. The pulse–echo method was used to measure the

---

D. Marshall—contributing editor

Manuscript No. 10330. Received June 23, 2003; approved August 29, 2003.
This work was supported by AIST, METI, Japan, as part of the Synergy Ceramics Project. Part of the work was supported by NEDO.

[†] Fine Ceramics Research Association.

[‡] National Institute of Advanced Industrial Science and Technology.

[★] Member, American Ceramic Society.

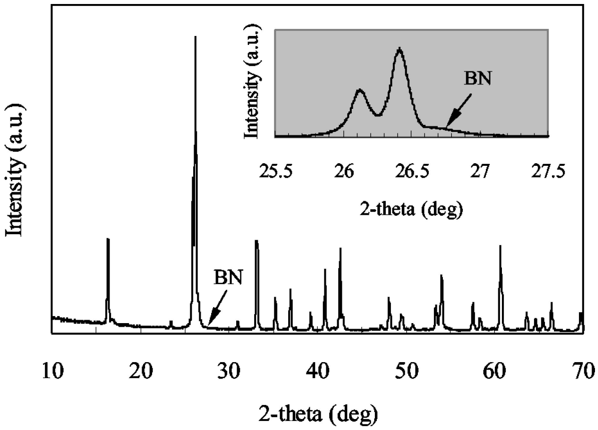

Fig. 1. XRD pattern of the mullite–BN composite RHPed at 1800°C. All peaks in this pattern are from the mullite phase. The inset pattern shows a broad peak ($2\theta = 26.6°$) for the BN phase with specialized diffraction in the angle range of 25.5–27.5°.

Young's modulus and the Poisson's ratio.[20] Scanning electron microscopy (SEM) observation of the fracture surface was conducted at 20 kV with a JSM-5600 (JEOL, Tokyo, Japan), and transmission electron microscopy (TEM) analysis of the microstructure was conducted at 300 kV with a Hitachi H-9000UHR III (Hitachi Co. Ltd., Tokyo, Japan).

III. Results and Discussion

The XRD pattern of the obtained composite RHPed at 1800°C is shown in Fig. 1. The other two composites RHPed at 1600° and 1700°C demonstrate similar XRD patterns. All peaks in this pattern are from the mullite phase. However, we can find a broad peak ($2\theta = 26.6°$) for the BN phase as shown in the inset pattern in this figure with specialized diffraction in the angle range of 25.5–27.5°. It pointed out that the in-situ-formed BN phase was in poor crystallinity.

The characteristics of the obtained composites are listed in Table I. From the relative density values we can find that the existence of the BN phase prohibited the densification of the composites. Nevertheless, the specimen RHPed at 1800°C demonstrated a high relative density of 98.3%. Because of the incomplete densification in the composites RHPed at 1600° and 1700°C, the main comparison will be made between the mullite–BN composite RHPed at 1800°C and the monolithic mullite.

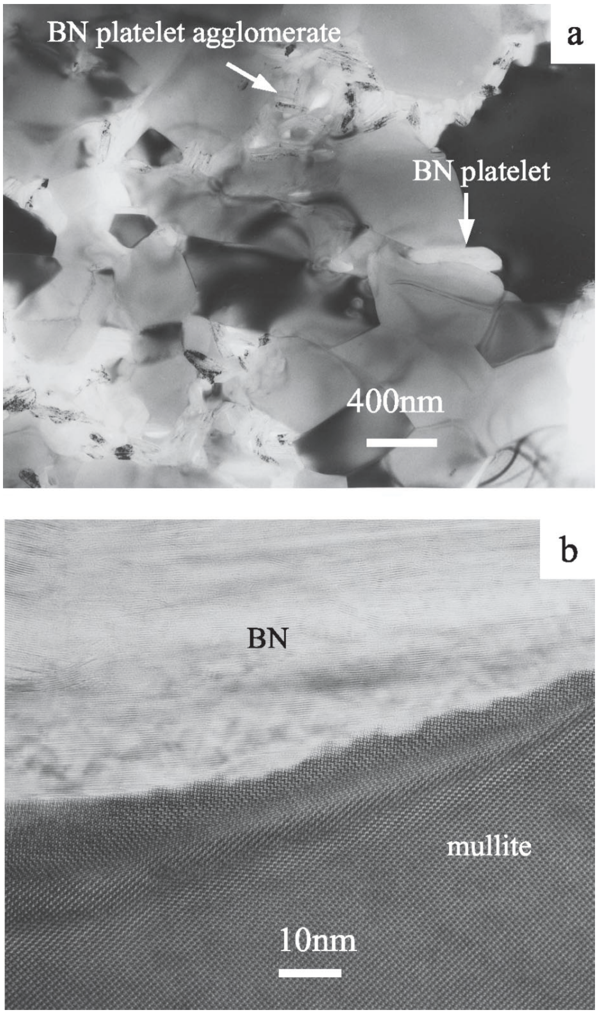

Fig. 2. TEM photographs of the obtained composite RHPed at 1800°C. The hot-press direction is vertical in the pictures. (a) Showing the whole distribution of the component phases of mullite and h-BN. (b) Demonstrating an example of the clean interface between an in-situ-formed h-BN platelet and a mullite grain.

The bending strength and Young's modulus for monolithic mullite were basically the typical ones published in the open literature. The toughness measured by the indentation technique was something lower than the typical data of 2–3 MPa·m$^{1/2}$ reported in the literature. On the other hand, however, the composite RHPed at 1800°C showed a very high bending strength of 540 MPa, which was 1.64 times, and a low Young's modulus of 153 GPa, which was 70% of that of the mullite monolithic, respectively. Thus, a high value of calculated strain to failure, which was 2.34 times higher than that of the mullite monolithic, was obtained. Accordingly, the present approach revealed that by the incorporation of the h-BN phase into the mullite matrix through the in-situ process mullite composites with improved strength and reduced elasticity could be realized. In addition, the toughness was a little higher than that of the mullite monolithic. Here we used different indentation load for measuring the toughness, and an early investigation showed that the load effect in the present load range was small.[21] This slight toughening effect (10% increment) in the composite might be resulted from the crack deflection or crack blunting by the weak or soft h-BN particles.

Table I. Characteristics of the Reactive Hot-Pressed Mullite–BN Composites

Property	RHPed at 1600°C	RHPed at 1700°C	RHPed at 1800°C	Mullite HPed at 1700°C
Phase composition	Mullite, BN	Mullite, BN	Mullite, BN	Mullite
Relative density	87.8	94.4	98.3	98.1
Strength (MPa)	230 ± 20	391 ± 71	540 ± 45	330 ± 54
Young's modulus (GPa)	107	147	153	218
Toughness (MPa·m$^{1/2}$)	1.4	1.8	1.7	1.6
Vickers hardness (GPa)	4.2	6.2	6.9	10.3
Poisson's ratio	0.19	0.21	0.21	0.27
Strain to failure ($\times 10^{-3}$)	2.15	2.66	3.53	1.51

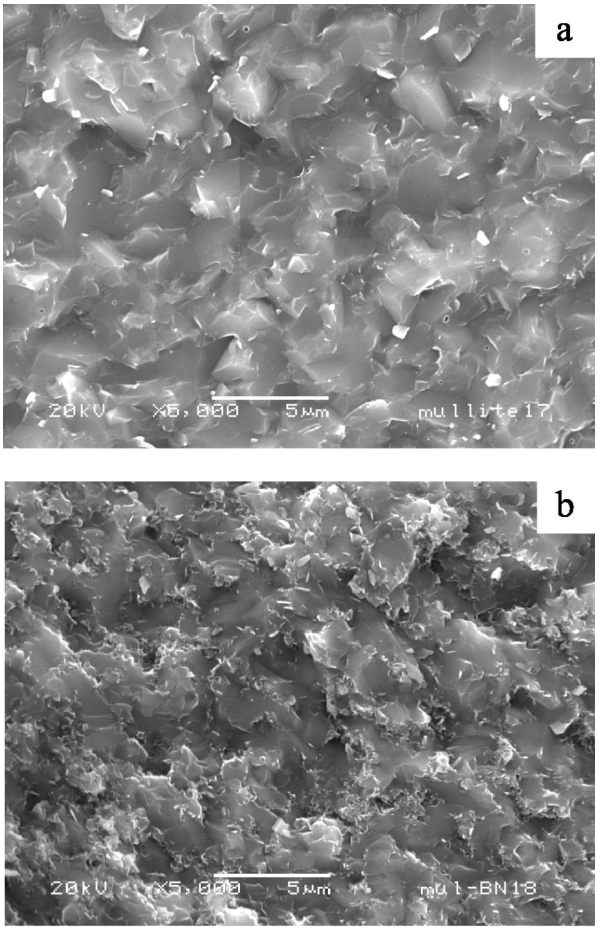

Fig. 3. Fracture surfaces of (a) monolithic mullite and (b) the composite RHPed at 1800°C. The hot-press direction is vertical in these pictures.

Accordingly, improved thermal shock resistance to fracture initiation can be reasonably expected.

Concerning the other properties, the composite showed a hardness value obviously lower than that of the mullite monolithic, due to the incorporation of the soft h-BN phase. In addition, the composite had a low Poisson's ratio compared with that of the mullite monolithic, and with the increase of porosity in the composites a decreasing trend in the Poisson's ratio could be found.

Figure 2 shows the TEM photographs of the obtained composite RHPed at 1800°C. We can find that the microstructure is isotropic without preferential orientation in either mullite or h-BN grains (Fig. 2(a)). The grain size of the matrix mullite is less than 1 μm in the image. The reaction-formed h-BN particles are in platelet shape with a length of about 200 nm and a thickness of 60–80 nm. These nanosized BN platelets are mainly in agglomerate shape of several platelets locating at the pockets formed by the mullite grains. These pockets are in general discrete. In some area single BN platelets also locate at the grain boundaries of the mullite matrix. There are almost no BN particles locating inside the mullite grains. The interfaces between BN platelets and mullite grains are very clean without an obvious amorphous phase. Figure 2(b) is an example of such clean interfaces, which is a very common feature in in-situ-reaction-synthesized composites.

The fracture surfaces of the composite RHPed at 1800°C and monolithic mullite are shown in Fig. 3. The intrafracture mode is dominant in these two materials, indicating that the grain-boundary bonding of the mullite matrix grains is still strong in the mullite–BN composite. It seems that the incorporation of the BN phase at the present fraction level does not weaken the grain network of the mullite matrix. Moreover, the composite is strengthened by the BN phase through reduction of the matrix grain size and the small toughening affect. It should be noted here that the distribution and particle size of the weak platelet-shaped h-BN phase is the critical point for obtaining high-strength composites. Formation of a weak h-BN network or the existence of large h-BN platelets will obviously degrade the material strength.[13,20]

In summary, a mullite–BN composite with a high strength of 540 MPa and a low elasticity of 153 GPa was fabricated by RHP based on a proposed reaction of aluminum borates and silicon nitride. The composite demonstrated an isotropic microstructure with a fine matrix grain size of less than 1 μm and nanosized h-BN platelets of about 200 nm in length and 60–80 nm in thickness.

Acknowledgments

The authors are members of the Joint Research Consortium of Synergy Ceramics.

References

[1] S. Kanzaki, H. Tabata, T. Kumazawa, and S. Ohta, "Sintering and Mechanical Properties of Stoichiometric Mullite," *J. Am. Ceram. Soc.*, **68** [1] C-6–C-7 (1985).

[2] J. F. Bartolome, M. Diaz, and J. S. Moya, "Influence of the Metal Particle Size on the Crack Growth Resistance in Mullite–Molybdenum Composites," *J. Am. Ceram. Soc.*, **85** [11] 2778–84 (2002).

[3] S. Wu and N. Claussen, "Reaction Bonding and Mechanical Properties of Mullite/Silicon Carbide Composites," *J. Am. Ceram. Soc.*, **77** [11] 2898–904 (1994).

[4] J. F. Bartolome, M. Diaz, J. Requena, J. S. Moya, and A. P. Tomsia, "Mullite/Molybdenum Ceramic–Metal Composites," *Acta Mater.*, **47**, 3891–99 (1999).

[5] N. Claussen and J. Jahn, "Mechanical Properties of Sintered, in Situ-Reacted Mullite–Zirconia Composites," *J. Am. Ceram. Soc.*, **63** [3–4] 228–29 (1980).

[6] A. Khan, H. M. Chan, M. P. Harmer, and R. F. Cook, "Alumina Agglomerate Effects on Toughness-Curve Behavior of Alumina–Mullite Composites," *J. Am. Ceram. Soc.*, **83** [12] 3089–94 (2000).

[7] Y. X. Huang, A. M. R. Senos, and J. L. Baptista, "Thermal and Mechanical Properties of Aluminum Titanate–Mullite Composites," *J. Mater. Res.*, **15**, 357–63 (2000).

[8] B. H. Mussler and M. W. Shafer, "Preparation and Properties of Mullite–Cordierite Composites," *Am. Ceram. Soc. Bull.*, **63** [5] 705–10 (1984).

[9] H. R. Rezaie, W. M. Rainforth, and W. E. Lee, "Fabrication and Mechanical Properties of SiC Platelet Reinforced Mullite Matrix Composites," *J. Eur. Ceram. Soc.*, **19**, 1777–87 (1999).

[10] D. D. Jayaseelan, D. A. Rani, T. Nishikawa, H. Awaji, and T. Ohji, "Sintering and Microstructure of Mullite–Mo Composites," *J. Eur. Ceram. Soc.*, **22**, 1113–17 (2002).

[11] Y. Shigegaki, M. E. Brito, K. Hirao, M. Toriyama, and S. Kanzaki, "Strain Tolerant Porous Silicon Nitride," *J. Am. Ceram. Soc.*, **80** [2] 495–98 (1997).

[12] Y. Inagaki, T. Ohji, S. Kanzaki, and Y. Shigegaki, "Fracture Energy of an Aligned Porous Silicon Nitride," *J. Am. Ceram. Soc.*, **83** [7] 1807–809 (2000).

[13] G. J. Zhang and T. Ohji, "In Situ Reaction Synthesis of SiC–BN Composites," *J. Am. Ceram. Soc.*, **84** [7] 1475–79 (2001).

[14] G. J. Zhang, Y. Beppu, T. Ohji, and S. Kanzaki, "Reaction Mechanism and Microstructure Development of Strain Tolerant In Situ SiC–BN Composites," *Acta Mater.*, **49**, 77–82 (2001).

[15] J. F. Yang, G. J. Zhang, N. Kondo, and T. Ohji, "Synthesis and Properties of Porous Si_3N_4/SiC Nanocomposites by Carbothermal Reaction between Si_3N_4 and Carbon," *Acta Mater.*, **50**, 4831–40 (2002).

[16] Z. Y. Deng, T. Fukasawa, M. Ando, G. J. Zhang, and T. Ohji, "Microstructure and Mechanical Properties of Porous Alumina Ceramics Fabricated by the Decomposition of Aluminum Hydroxide," *J. Am. Ceram. Soc.*, **84** [11] 2638–44 (2001).

[17] W. S. Coblenz and D. Lewis, "In Situ Reaction of B_2O_3 with AlN and/or Si_3N_4 to Form BN-Toughened Composites," *J. Am. Ceram. Soc.*, **71** [12] 1080–85 (1988).

[18] G. J. Zhang, J. F. Yang, M. Ando, T. Ohji, and S. Kanzaki, "Reactive Synthesis of Alumina–Boron Nitride Composites," *Acta Mater.*, in review.

[19] "Testing Methods for Fracture Toughness of Fine Ceramics," Japanese Industrial Standard No. JIS R 1607, 1995.

[20] G. J. Zhang and T. Ohji, "Effect of BN Content on Elastic Modulus and Bending Strength of SiC–BN in Situ Composites," *J. Mater. Res.*, **15** [9] 1876–80 (2000).

[21] G. R. Anstis, P. Chantikul, B. R. Lawn, and D. B. Marshall, "A Critical Evaluation of Indentation Techniques for Measuring Fracture Toughness: I, Direct Crack Measurement," *J. Am. Ceram. Soc.*, **64** [9] 533–38 (1981). ☐